Phthaloylcobalt Complexes in Synthesis. Ligand Modifications Leading to a Practical Naphthoquinone Synthesis

Lanny S. Liebeskind,*[1,2] Sherrol L. Baysdon,[3] Virgil Goedken,*[3] and Ramakrishnan Chidambaram[2]

Departments of Chemistry, Emory University, Atlanta, Georgia 30322, and Florida State University, Tallahassee, Florida 32306

Received June 17, 1985

Modification of the ligands of trigonal-bipyramidal (phthaloyl)Co(PPh_3)$_2$Cl has led to an understanding of how this complex reacts with alkynes to give naphthoquinones when activated with $AgBF_4$. Through X-ray crystal structure determinations and temperature-dependent ^1H NMR spectra, it has been determined that reaction with alkynes requires conversion of (phthaloyl)Co(PPh_3)$_2$Cl into a six-coordinate complex with a dissociable ligand above or below the plane defined by the phthaloylcobalt ring. Treatment of (phthaloyl)Co(PPh_3)$_2$Cl with dimethylglyoxime in pyridine effects such a transformation in high yield, and the resulting air-stable complex (phthaloyl)Co(dimethylglyoxime)(pyridine)Cl reacts with alkynes at 80 °C to produce excellent yields of naphthoquinones. A simple synthesis of menaquinones has been realized by using this method. In addition, $SnCl_4$ has been shown to catalyze the quinone forming reaction at room temperature.

Introduction

Reaction of benzocyclobutenedione with ClCo(PPh_3)$_3$ gives the very stable five-coordinate bis(triphenylphosphine)phthaloylcobalt complex **1** in high yield.[4,5] As we have previously described, phthaloylcobalt complex **1** reacts with alkynes to give substituted naphthoquinones, but only when activated by treatment with ≥2 equiv of $AgBF_4$ (eq 1).[6] From the inception of this method for

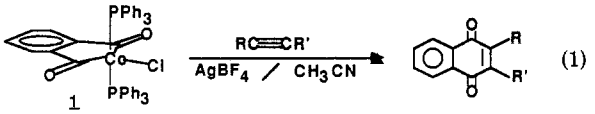

(1)

naphthoquinone synthesis, we have searched for a simple means of activating phthaloylcobalt complex **1** that would obviate the need for $AgBF_4$. Our knowledge of how $AgBF_4$ activated complex **1** for reaction with alkynes to produce naphthoquinones[5] led us to design a simple ligand modification of **1** which overcame the need for $AgBF_4$ in this reaction.

Background

We have previously shown that one equivalent of $AgBF_4$ in acetonitrile (AN) converted phthaloylcobalt complex **1** into the tris(acetonitrile)phthaloylcobalt cation **2**. Complex **2** reacted rapidly with alkynes to produce naphthoquinones in high yield provided a second equivalent of $AgBF_4$ was present in the reaction medium to coordinate to the free PPh_3 liberated during the reaction. In the absence of the second equivalent of $AgBF_4$, the yields of naphthoquinone product were diminished because the liberated PPh_3 reacted with cation **2** to give the stable bis(phosphine) complex **3** which did not react efficiently with alkynes (Scheme I). We proposed[5] that naphthoquinone formation occurred by prior complexation of the alkyne to one of the

Scheme I

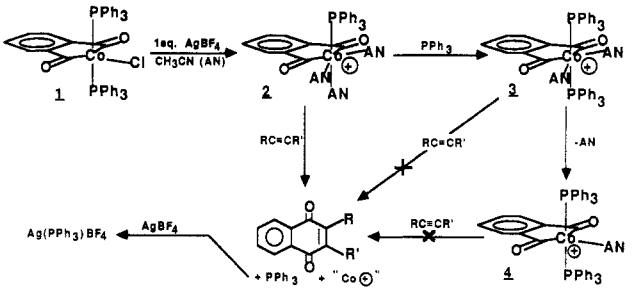

cobalt coordination sites above or below the plane of the phthaloyl ring (arbitrarily called axial sites throughout this manuscript). On the basis of this presumption, bis(phosphine) complex **1** was unreactive because PPh_3 dissociation was energetically unfeasible (16e → 14e) and alkyne coordination (16e → 18e) followed by ligand rearrangement was sterically inhibited. Bis(phosphine) cation **3** was unreactive because ligand dissociation, even though energetically reasonable (18e → 16e), was dominated by dissociation of an *equatorial* CH_3CN ligand to give the stable 5-coordinate bis(phosphine) cation **4**, itself unreactive toward alkynes for the same reasons given for complex **1**. Cobalt complex **2** *was* reactive in the naphthoquinone synthesis because it could free up an axial site for alkyne coordination by dissociating the weakly held axial CH_3CN ligand. These considerations led us to the synthesis of a chelated diphos complex {diphos = 1,2-bis(diphenylphosphino)ethane} which, on the basis of NMR studies at room temperature, was assigned the 5-coordinate structure **5** (eq 2).

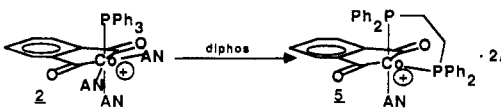

(2)

In accord with the previous hypothesis, the diphos complex reacted efficiently with alkynes to provide naphthoquinones because of the weak CH_3CN ligand in the apical position. On the basis of an X-ray structure determination, we now report that the diphos complex is actually a 6-coordinate species, and we describe our further studies of ligand modifications in the phthaloylcobalt series that have led us to a practical and efficient naphtho-

(1) Fellow of the Alfred P. Sloan Foundation, 1983–1987. Camille and Henry Dreyfus Teacher-Scholar, 1986–1991.
(2) Emory University
(3) Florida State University
(4) Liebeskind, L. S.; Baysdon, S. L.; South, M. S.; Blount, J. F. *J. Organomet. Chem.* **1980**, *202*, C73.
(5) Baysdon, S. L.; Liebeskind, L. S. *Organometallics* **1982**, *1*, 771.
(6) Liebeskind, L. S.; Baysdon, S. L.; South, M. S. *J. Am. Chem. Soc.* **1980**, *102*, 7397.

0276-7333/86/2305-1086$01.50/0

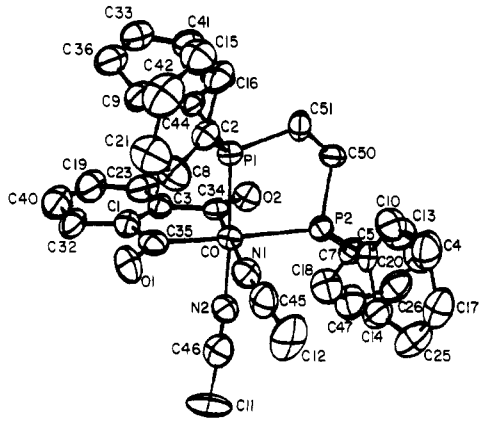

Figure 1. Ortep diagram of (phthaloyl)Co(diphos)$(CH_3CN)_2BF_4$ (**6**) showing 50% probability thermal elipsoids and the numbering scheme for the atoms. Bond distances (Å) around Co: Co–P1, 2.213 (3); Co–P2, 2.359 (3); Co–C34, 1.919 (10); Co–C35, 1.918 (10); Co–N1, 2.013 (10); Co–N2), 1.927 (10). Atoms N3, C48, and C52 (not shown) comprise the latice CH_3CN molecule.

quinone synthesis without the use of $AgBF_4$ for activation.

Results and Discussion

Crystals of the diphos complex suitable for X-ray crystallography were grown by slow diffusion of diethyl ether into a concentrated solution of the compound in hot CH_3CN. The Ortep diagram (and selected bond distances) shown in Figure 1 clearly establishes the 6-coordinate structure **6** for the diphos complex. Although the accuracy

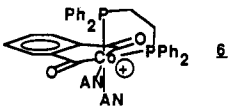

6

of the structure is lower than desirable, the trends of the bond distances within the coordination sphere agree with known trends regarding the trans effect in organocobalt (III) compounds: P(2) which is trans to C(35) has a longer Co–P distance, 2.359 Å, than the Co–P(1) distance, 2.213 Å, which is trans to an acetonitrile. Similarily, the acetonitrile trans to C(34) has a longer Co–N distance, 2.013 Å, than that which is trans to P(1), which has a Co-N distance of 1.927 Å. The Co–P distances are similar to that observed in $Co(dimethylglyoxime)_2(PPh_3)Cl$, 2.327 Å.[7] The third acetonitrile molecule associated with the diphos complex (not shown) is solvent of crystallization and can be removed under vacuum (0.1 mm) at 100 °C for 2 h.

The original assignment of structure **5** to the diphos complex was based on room-temperature ^{31}P NMR studies which showed two different kinds of coordinated phosphorus atoms (+43.11 and +38.35 ppm relative to 85% H_3PO_4) and on ^1H NMR studies which showed two different kinds of acetonitrile molecules, a three-proton absorption at 2.19 ppm (d, J = 2 Hz) and a six-proton absorption at 1.93 ppm (s) (these data were taken in $CDCl_3$ at 270 MHz while those reported in our earlier manuscript[5] were measured in CD_2Cl_2 at 60 MHz). However, lowering the temperature of the NMR probe to −64 °C resolved the absorptions into singlets at 1.94 and 2.13 ppm and a broad doublet (J = 2 Hz) at 2.32 ppm. The lower temperature spectrum is consistent with structure **6**, the doublet at 2.32 ppm assigned to the axial CH_3CN (coupled to the trans phosphorus) and the other absorptions originating from the equatorial CH_3CN (2.13 ppm) and a free CH_3CN (1.94 ppm). In structure **6** the equatorial CH_3CN should experience *some* anisotropic shielding from the adjacent PPh_2 group (see the Ortep of **6** and compare with the chemical shift of the CH_3CN in the CO complex **7** described below), but the exact extent of this phenomenon is unclear.

Analysis of the room-temperature ^1H NMR suggests a definite 5-coordinate appearance, but we reevaluate the data in terms of an equilibrium between the two equivalent 5-coordinate square-base pyramids shown below[8] rather than a static trigonal bipyramid as previously suggested. Support for this hypothesis is seen in the appearance of the apical CH_3CN at room temperature as a *coupled* three-proton absorbance (2.19 ppm, d, J = 2 Hz—rapid exchange of this ligand is precluded by the appearance of coupling to phosphorus), with two equivalent free CH_3CN ligands absorbing as a six-proton singlet at 1.93 ppm, while the ethylene bridge protons of the diphos ligand appear as a symmetrical, but significantly broadened absorption centered near 3 ppm. These data require that, at room temperature, the molecule be fluxional in such a way that the apical CH_3CN does not lose its coupling to phosphorus and that its environment not be changed, while the diphos ethylene backbone has not become completely symmetrized on the NMR time scale. The appearance of the room-temperature spectrum requires that the molecule is not a true trigonal bipyramid with free CH_3CN ligands, nor is it equilibrating between two equivalent six-coordinate species **6** by an S_N2-like displacement of the equatorial CH_3CN with a noncoordinated CH_3CN (the six-proton singlet would appear halfway between the chemical shifts of the exchanging ligands—2.04 ppm). At higher temperatures, the NMR spectra begin to show coalescence of all of the acetonitriles, while the diphos ligand absorptions resolve to a symmetrical pattern expected for the trigonal-bipyramidal structure originally suggested for **6**. In total, the temperature-dependent ^1H NMR data suggest a facile equilibrium between 6- and 5-coordinate species with the position of the equilibrium lying on the 6-coordinate side at low temperature and on the 5-coordinate side at higher temperature. Equatorial ligand dissociation predominates; however, the data do not preclude a *kinetically significant* role for axial ligand dissociation. The shift from a 6-coordinate structure at low temperature to a 5-coordinate structure at higher temperature is consistent with a dominant role for the $T\Delta S$ term of the free energy difference for the equilibrium between the 6- and 5-coordinate species.

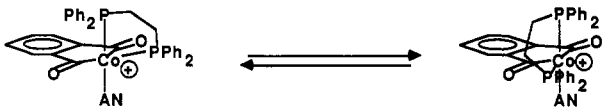

Consistent with the discussed hypothesis of axial alkyne coordination, the excellent reactivity of 6-coordinate diphos complex **6** with alkynes[5] can be rationalized by axial CH_3CN dissociation (18e → 16e) followed by alkyne coordination. On the basis of the ^1H NMR data described above, we expect that a facile equilibrium between 5- and 6-coordinate species exists, dominated by loss of the equatorial ligand but with a *kinetically significant* dissociation of the axial CH_3CN. The lability of the axial CH_3CN ligand was demonstrated by reaction of diphos cation **6** with CO (1 atm) in CH_2Cl_2 at room temperature to provide the 6-coordinate CO complex **7** in 92% yield (eq 3). Assignment of the CO to the axial site and the CH_3CN to the equatorial site was based on the absence of phosphorus coupling to the CH_3CN and on the high-

(7) Bresciani-Pahor, N.; Calligaris, M.; Randaccio, L.; Marzilli, L. G. *Inorg. Chim. Acta* **1979**, *32*, 181.

(8) Hoffman, P. R.; Caulton, K. G. *J. Am. Chem. Soc.* **1975**, *97*, 4221.

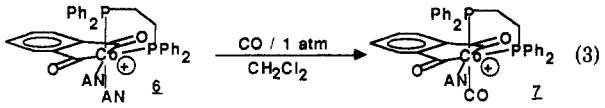

(3)

field chemical shift of the CH_3CN ligand (1.57 ppm in $CDCl_3$, presumably anisotropically shielded by the adjacent phenyl rings of the diphos ligand).

Establishment of 6-coordinate structures with weakly held axial ligands for both of the reactive phthaloylcobalt species (**2** and **6**) suggested to us that incorporation of a *chelating* ligand in the plane of the phthaloyl ring of complex **1** might accomplish the same activating function as the $AgBF_4$. The transformation of **1** into a 6-coordinate complex with a chelating ligand in the plane of the phthaloyl ring (eq 4) should (1) facilitate ligand dissocia-

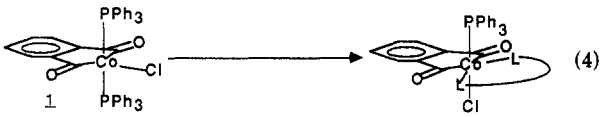

(4)

tion (18e → 16e easier than 16e → 14e), (2) inhibit equatorial ligand dissociation (chelate effect), and (3) leave only an axial ligand free to dissociate. If the premise of alkyne coordination in an axial site is correct, then these chelate complexes should show reactivity with alkynes under strictly thermal conditions and obviate the need for $AgBF_4$ in this chemistry.

After a wide variety of chelating ligands were surveyed, we finally discovered that dimethylglyoxime fulfilled our requirements perfectly. Treatment of **1** with 1.1 equiv of dimethylglyoxime in refluxing acetonitrile gave a quantitative yield of **8** as a greenish gold solid (eq 5). If a similar reaction was conducted in pyridine at room temperature for 12 h, 88% of the yellow-brown pyridine analogue **9** was obtained (eq 5). Although requiring two steps, we found

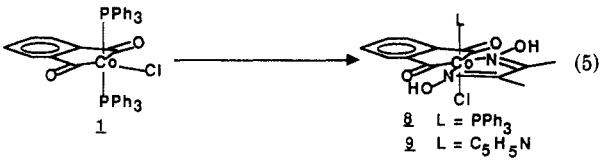

(5)

that the alternative procedure of treating **1** with excess pyridine gave an insoluble orange precipitate (infrared analysis suggests a bis(pyridine) analogue of **1**) and subsequent treatment of the precipitate with 1.1 equiv of dimethylglyoxime (based on the amount of **1** used) in refluxing acetonitrile reproducibly provided 95% yield of pure **9**. Six-coordinate, equatorially chelated structures for both complexes were suggested by the ^1H NMR spectra that, in each case, showed one absorption for the OH protons (13.59 ppm for **8** and 13.76 ppm for **9**), one absorption for the CH_3 groups (2.01 ppm for **8** and 2.32 ppm for **9**), and symmetrical patterns for all remaining protons.

Confirmation of the equatorial disposition of the chelating dimethylglyoxime ligand was obtained through an X-ray crystal structure determination on the pyridine analogue **9**. Crystals of **9** suitable for X-ray crystallography were grown by diffusion of diethyl ether into a concentrated solution of **9** in hot CH_3CN. The crystal structure of Co(DMG)(phthaloyl)Cl(pyridine) consists of two crystallographically independent, but chemically equivalent, molecules of **9**. There are no significant differences in the bond parameters of the two independent molecules. The Ortep diagram (with the labeling scheme for one of the molecules and selected bond distances) shown in Figure 2 clearly established the anticipated structure. The phthaloyl dianion is one of the few chelating carbon-donor ligands that we are aware of that has been structurally

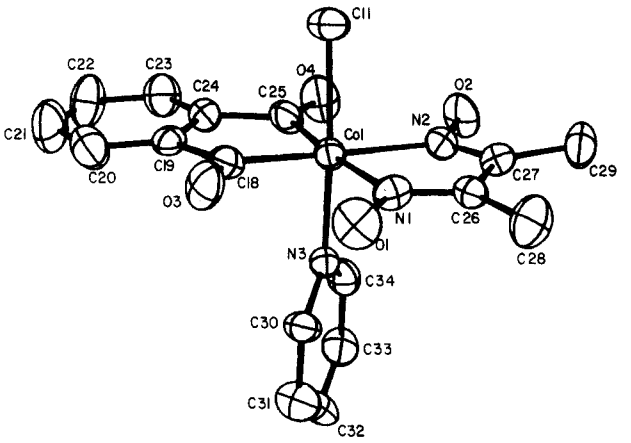

Figure 2. Ortep plot of (phthaloyl)Co(dmg)(pyridine)Cl (**9**) showing 50% probability thermal ellipsoids and numbering scheme for one of the two independent molecules of the unit cell. Bond distances (Å) around Co: Co1–Cl1, 2.251 (2); Co1–N1, 2.015 (6); Co1–N2, 2.026 (6); Co1–N3, 1.960 (6); Co1–C18, 1.871 (8); Co1–C25, 1.860 (8).

characterized, but the complex superfically resembles the well-characterized Co^{III}DMG complexes.[9,10] The hydrogen bonding between the dimethylglyoxime ligand and the phthaloyl ligand provides an identifiable source of stabilization of the planar arrangement similar to the bis(dimethylglyoxime) complexes. The strong σ-donor carbon atoms trans to the π-acceptor α-diimine linkage may provide some electronic stabilization, but the structural parameters do not support the notion of such an effect; rather the traditional view of carbanions as exerting strong trans labilizing influences is confirmed. The Co–C distances average 1.866 Å (approximately 0.1 Å shorter than observed for aliphatic Co–C distances[11–13]), and the Co–N(imine) bonds are considerably longer than in bis(dimethylglyoximato) complexes of Co(III).[9,10] The average Co–N distance for the two molecules, 2.016 Å, is a full 0.1 Å longer than in other Co(III) dimethylglyoxime complexes (average 1.90 Å) indicating a substantial trans-lengthening effect from the phthaloyl ligand. The Co–Cl and Co–pyridine distances are normal for Co(III) structures.

Reaction of the dimethylglyoxime–pyridine complex **9** with alkynes was investigated. Heating a CH_2Cl_2 or dichloroethane solution of **9** and 3-hexyne (1.5 equiv) in a sealed tube for 18 h gave 2,3-diethyl-1,4-naphthoquinone in 77% yield. A similar reaction with 1-hexyne produced 2-*n*-butyl-1,4-naphthoquinone in 85% yield. These reactions strongly support our previous mechanistic rationale requiring dissociation of an axial ligand. In an effort to decrease the reaction time, we investigated the effect of a number of additives on the reaction of **9** with 3-hexyne at 80 °C (Table I). Strong Lewis acids such as $AgBF_4$ (entry 2) and $BF_3{\cdot}Et_2O$ (entry 3) gave very good yields of quinone in reaction times much shorter than the control run (entry 1). Cobalt chloride, either anhydrous or hydrated, also had a significant influence on the reaction rate (entries 4 and 5), and the use of the hydrate demonstrated that the reaction was not adversely affected by the presence of water. The successful catalysis of the 80 °C reaction suggested that reaction at room temperature might

(9) Crumbliss, A. L.; Bowman, J. T.; Graus, P. L.; McPhail, A. T. *J. Chem. Soc., Chem. Commun.* **1973**, 415.
(10) Bigotto, A.; Zangrando, E.; Randaccio, L. *J. Chem. Soc., Dalton Trans.* **1976**, 96.
(11) Pratt, J. M.; Craig, P. J. *Adv. Organomet. Chem.* **1973**, *11*, 331.
(12) Calligaris, M.; Nardin, G.; Randaccio, L. *J. Chem. Soc., Dalton Trans.* **1972**, *1433*.
(13) Marzilli, L. G.; Toscano, P. J.; Randaccio, L.; Bresciani-Pahor, N.; Calligaris, M. *J. Am. Chem. Soc.* **1979**, *101*, 6754.

Table I. Effect of Additives on 2,3-Diethyl-1,4-naphthoquinone Formation at 80 °C

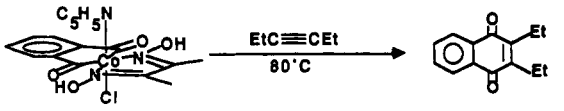

additive (1 equiv)	GC yield, % 2 h	5 h	18 h
none	25	52	77
$AgBF_4$	80	82	...
$BF_3{\cdot}Et_2O$	74	79	82
$SnCl_2$	41	39	70
$CoCl_2{\cdot}6H_2O$	59	83	91
$CoCl_2$ (anhyd)	61	86	86
p-CH_3PhSO_3H	14	31	76
CH_3CO_2H	23	47	74

Table II. Effect of Lewis Acids on 2-*n*-Butyl-1,4-naphthoquinone Formation at 25 °C

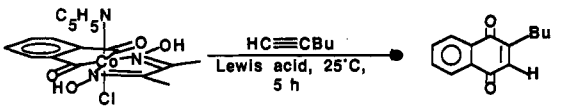

Lewis acid	isolated yield, %	Lewis acid	isolated yield, %
$SnCl_4$	76	$ZnCl_2$	40
$TiCl_4$	31	$FeCl_3$	28
$BF_3{\cdot}Et_2O$	39	$AgBF_4$	76
$MgBr_2{\cdot}Et_2O$	0		

be possible in the presence of a proper Lewis acid. To probe this possiblity, we surveyed the reaction of **9** with 1-hexyne in dichloroethane at *room temperature* in the presence of a variety of Lewis acids (Table II). These results demonstrate the unique ability of $SnCl_4$ as well as $AgBF_4$ to catalyze the room-temperature formation of quinones from **9**.

In order to assess the generality of quinone formation from this new class of phthaloylcobalt complex, we surveyed the reaction of **9** with a number of alkynes using $CoCl_2{\cdot}6H_2O$ for catalysis at 80 °C and $SnCl_4$ at room temperature (Table III). Successful application of this chemistry (with or without added Lewis acid) requires attention to two details. First, to a varying degree depending on the substrate, reduction to the hydroquinone occurs under the reaction conditions. In order to free the hydroquinone product, an acidic workup is required. Second, an oxidative treatment of the crude reaction mixture will be necessary to convert all product to the quinone oxidation state, unless air oxidation is a facile process. The later circumstance prevails for simple alkyl-substitued naphthohydroquinones. From the entries in Table III it can be seen that high yield quinone formation is a general phenomenon with alkynes ranging from electron rich to electron poor. The cobalt chloride catalyzed variant is perfectly resonable for most applications, while the $SnCl_4$ system should find use where lower temperature reactions are advantageous. The electron-rich alkyne ethyl-1-propyne was not compatible with the stongly Lewis acidic conditions of the $SnCl_4$ system. Included in this table are simple, high-yield syntheses of the menaquinones[14] MK-1 and MK-2 (last two entries), which underscore the simplicity of the method. Syntheses of the required alkynes are described in the Experimental Section. These cumulative results show that the dimethylglyoxime variant of our phthaloylcobalt complex is the most generally reactive system we have prepared to date.

(14) For a recent reference to menaquinone synthesis see: Naruta, Y. *J. Am. Chem. Soc.* **1980**, *102*, 3774.

Table III. Synthesis of Naphthoquinones

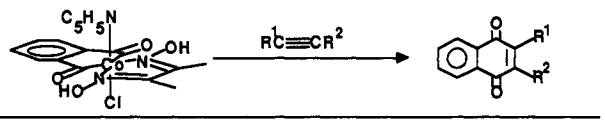

R^1	R^2	isolated yield, % $CoCl_2{\cdot}6H_2O$, 80 °C, 8 h	$SnCl_4$, room temp, 7 h
n-Bu	H	87	80
Et	Et	86	83
Me	CO_2Et	99	80
Et	OEt	85	0
Me	*t*-Bu	72	...
Me	CH_2CHCMe_2	94	...
Me	(E,E)-$[CH_2CHCMeCH_2]_2H$	86	...

In theory **9** could acquire the coordinative unsaturation necessary for reaction with alkynes by dissociation of the axial pyridine ligand or by ionization of the axial chloride ligand, or by a combination of both processes. Pyridine dissociation was firmly established by the following two experiments. Treatment of pyridine complex **9** with excess PPh_3 in refluxing CH_3CN (15 min) gave, after cooling to room temperature and slowly adding Et_2O, the previously prepared PPh_3 compound **8** in 86% yield (eq 6). Reaction

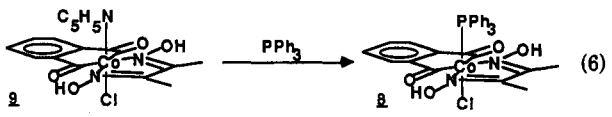

(6)

of **9** with 1 equiv of $Et_4N^+Cl^-$ in acetone at room temperature for 72 h gave a deep red precipitate that was assigned structure **10** based upon IR, ^1H NMR, and elemental analysis (eq 7). The first experiment suggests a

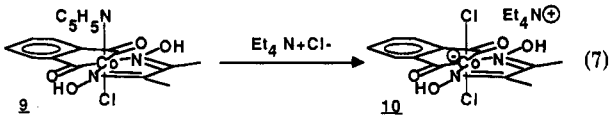

(7)

direct pyridine dissociation pathway for **9** while the second experiment requires it.

These results point to pyridine dissociation as one means for alkyne coordination, but they do not rule out chloride ionization as an equally probable, or even dominant pathway. The high-field ^1H NMR spectrum of analytically pure, recrystallized **9** consistently showed traces (ca. 5%) of a second type of pyridine molecule that absorbed slightly *downfield* of the three sets of absorptions of the coordinated pyridine (ortho, meta, and para hydrogens) of **9**. We confirmed that the small absorptions were *not* due to free pyridine and suggest that the downfield shift of these peaks is consistent with the ionization equilibrium shown in eq 8. In fact, the extremely rapid quinone formation

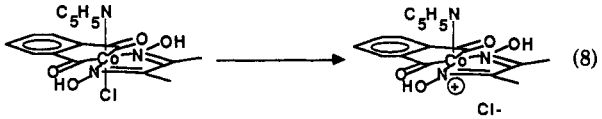

(8)

observed when **9** was activated with $AgBF_4$ (Table I, entry 2, and Table II, entry 7) lends further support to this hypothesis. Furthermore, the wide variability in the efficacy of catalysis by the Lewis acids shown in Table II suggests that chloride ionization might be the main pathway for the room-temperature reactions. If pyridine dissociation were occurring to a significant extent at room temperature, most of the Lewis acids should have shown a significant catalytic effect by strongly binding the liberated pyridine. The fact that $SnCl_4$ and $AgBF_4$ are so

effective at catalysis of the quinone formation suggests that the room-temperature reaction is activated by Lewis acids that can facilitate chloride ionization ($Ag^+ \rightarrow AgCl$ and $SnCl_4 \rightarrow SnCl_5^{1-}$ or $SnCl_6^{2-}$). Additional studies with ionic ligands other than chloride will be required to establish the ionization pathway.

Conclusions

A very practical and general method for quinone synthesis has been developed by using transition-metal species by paying close attention to the coordination chemistry of the intermediates. The chemistry in this manuscript and in our previous publications emphasizes the dominant role that auxiliary ligands can play in converting an interesting synthetic observation into a practical synthetic method. This approach to developing synthetic organic reactions using organo-transition-metal chemistry should prove useful in other systems. Our current efforts in this quinone chemistry are focussed on establishing good regioselectivity with unsymmetrical substrates.

Experimental Section

General Methods. All melting points were obtained on a Mel-Temp melting point apparatus and are uncorrected. Infrared spectra were taken on a Perkin-Elmer Model 1320 spectrophotometer, and absorptions are reported in wavenumbers. ^1H NMR spectra were taken at 200 MHz on a IBM NB 200 SY FT spectrometer, at 270 MHz on a IBM NB 270 SY FT spectrometer, and at 360 MHz on a Nicolet NMC-360 spectrometer. All NMR absorptions are expressed in parts per million (δ) relative to tetramethylsilane as an internal standard. Low-resolution electron-impact mass spectra were obtained on a Finnigan 4510 GC/MS system by a direct insertion probe. Gas–liquid chromatography was performed on a Varian 3700 instrument equipped with flame ionization detectors using a 6 ft × 0.25 in. glass column packed with 3% OV-101 on 80/100 Chrom W-HP. GLC yields were calculated from peak areas obtained with a Hewlett-Packard 3380 S recording integrator using internal standard techniques. Thin-layer chromatography was effected on E. Merck silica gel 60 F-254 glass-backed plates of 0.25-mm thickness, and visualization was performed with appropriate combinations of UV light, $KMnO_4$ stain, and phosphomolybdic acid stain. Preparative plate chromatography was done on E. Merck silica gel 60 F-254 glass backed plates of 2.0 mm thickness. Gravity column chromatography was performed by using Baker SiO_2, 60–200 mesh. Unless otherwise indicated, all reactions were carried out under an atmosphere of dry, prepurified nitrogen. Sealed tube reactions were performed in heavy-walled glass reaction tubes with a two-piece threaded aluminum coupling and an internal Teflon sealing disk (available from Regis Chemical Co.) or in pressure tubes with Ace-thread Teflon screw caps (available from Ace Glass Inc.). Elemental analyses were performed by Gailbraith Laboratories, Knoxville, TN.

Materials. Diethyl ether and tetrahydrofuran were purified by distillation from sodium–benzophenone under nitrogen. Acetonitrile, CH_2Cl_2, and $C_2H_4Cl_2$ were purchased reagent grade and then purified by passage through E. Merck activity 1 alumina. Commercially available alkynes were purchased from Farchan Chemicals and passed through a short plug of alumina before use. Phthaloylcobalt complexes **1–6** (**5** = **6**) were prepared as described in reference.[5]

Collection of X-ray Diffraction Details and Solution of the Crystal Structure of (Phthaloyl)Co(diphos)-$(CH_3CN)_2BF_4$·CH_3CN (6). Single crystals of $CoC_{40}H_{37}P_2BF_4N_3O_2$ (**6**) were grown by dissolving a sample in a minimum of hot CH_3CN and allowing Et_2O to slowly diffuse into the CH_3CN solution. The experimental data for the X-ray diffraction study are given in Table IV. No absorption correction was necessary (μ = 5.86 cm^{-1}). Intensities of three standard reflections were measured every 2 h. Appreciable anistropic crystal decomposition occurred during the data collection with the intensity of one of the standard reflections falling to 85% of its initial value. The intensity data were scaled, based on the average decrease in intensity of the standard reflections, to account for the crystal decay. The structure was solved by Patterson and Fourier

Table IV. Crystal Data for 6

formula	$CoC_{40}H_{37}P_2BF_4N_3O_2$	cryst color	orange
mol wt	800.65	radiatn	Mo Kα
cryst dim. (mm)	0.15 × 0.20 × 0.30	diffractometer	Enraf-Nonius CAD-4
cryst syst	triclinic	abs coeff, cm^{-1}	5.86
a, Å	11.723 (7)	space group	$P\bar{1}$
b, Å	12.555 (8)	scan speed, deg/min	variable (2–10)
c, Å	14.658 (8)	2θ scan range, deg	1–45
α, deg	81.36	scan technique	θ–2θ
β, deg	78.80	data collected	6990
γ, deg	65.03	scan width, deg	2
V, Å^3	1912.8 (2)	unique data with $I > 2\sigma(I)$	4593
Z	2	std rflctns	3
d(calcd), g·cm^{-3}	1.39	LS parameters	540
d(obsd), g·cm^{-3}	1.40	R, % (F_o)	7.3
		R_w, % (F_o)	9.0

Table V. Bond Angles and Distances of 6

	Distances (Å)		
Co–P1	2.213 (3)	C14–C25	1.39 (1)
Co–P2	2.359 (3)	C15–C16	1.39 (1)
Co–C34	1.919 (10)	C15–C42	1.38 (1)
Co–C35	1.918 (10)	C17–C25	1.35 (1)
Co–N1	1.013 (10)	C18–C47	1.41 (1)
Co–N2	1.927 (10)	C19–C23	1.39 (1)
C1–C3	1.38 (1)	C19–C40	1.41 (1)
C1–C32	1.37 (1)	C20–C28	1.37 (1)
C1–C35	1.49 (1)	C21–C42	1.35 (1)
C2–C8	1.40 (1)	C28–C47	1.38 (1)
C2–C16	1.38 (1)	C32–C40	1.39 (1)
C3–C23	1.38 (1)	C33–C36	1.36 (1)
C4–C10	1.38 (1)	C33–C41	1.36 (1)
C4–C17	1.37 (1)	C34–O2	1.23 (1)
C5–C10	1.38 (1)	C35–O1	1.23 (1)
C5–C14	1.40 (1)	C36–C33	1.36 (1)
C7–C13	1.37 (1)	C37–C41	1.40 (1)
C7–C18	1.37 (1)	C37–C44	1.40 (1)
C8–C21	1.37 (1)	N1–C45	1.14 (1)
C9–C36	1.40 (1)	C45–C12	1.43 (1)
C9–C44	1.40 (1)	N2–C46	1.16 (1)
C13–C20	1.43 (1)	C46–C11	1.47 (1)
	Angles (deg)		
	Around Cobalt		
P1–Co–C35	91.8 (5)	P2–Co–C34	91.1 (5)
P2–Co–N2	96.0 (5)	P1–Co–C34	87.0 (5)
P1–Co–N2	175.4 (5)	P2–Co–N1	88.5 (5)
P1–Co–P2	87.5 (3)	P1–Co–N1	95.1 (5)
P2–Co–C35	177.0 (5)	C34–Co–C35	85.9 (6)
C35–Co–N1	94.5 (5)	C34–Co–N1	177.8 (6)
C35–Co–N2	84.6 (6)	C34–Co–N2	90.0 (6)
N1–Co–N2	87.9 (6)		
	Within Ligands		
C3–C1–C32	121.3 (6)	C23–C19–C40	119.4 (6)
C3–C1–C35	113.9 (6)	C13–C20–C28	118.8 (6)
C32–C1–C35	124.7 (6)	C8–C21–C42	120.6 (6)
C8–C2–C16	118.7 (7)	C3–C23–C19	118.3 (7)
C1–C3–C23	121.7 (6)	C14–C25–C17	121.4 (6)
C1–C3–C34	114.8 (6)	C20—C28–C47	121.1 (7)
C23–C3–C34	123.5 (7)	C1–C32–C40	117.6 (6)
C10–C4–C17	119.7 (7)	C36–C33–C41	119.2 (6)
C10–C5–C14	118.0 (6)	C3–C34–O2	121.9 (6)
C13–C7–C18	116.9 (6)	C12–C35–O1	121.0 (6)
C2–C8–C21	120.4 (6)	C9–C36–C33	122.0 (6)
C36–C9–C44	118.7 (6)	C41–C37–C44	119.7 (7)
C4–C10–C5	121.1 (6)	C19–C40–C32	121.6 (7)
C7–C13–C20	123.2 (6)	C33–C41–C37	121.3 (7)
C5–C14–C25	119.7 (6)	C15–C42–C21	120.3 (7)
C16–C15–C42	119.6 (6)	C9–C44–C37	119.1 (7)
C2–C16–C15	120.3 (6)	N1–C45C12	176.9 (7)
C4–C17–C25	120.2 (6)	N2–C46–C11	178.3 (8)
C7–C18–C47	122.8 (6)	C18–C47–C28	117.1 (7)

Table VI. Crystal Data for 9

formula	$CoC_{17}ClN_3O_4H_{17}$	radiatn	Mo Kα
mol wt	433.8	diffractometer	Enraf-Nonius CAD-4
cryst dimns, mm	0.20 × 0.20 × 0.25	abs coeff, cm^{-1}	11.3
cryst syst	monoclinic	scan speed, deg/min	variable (2–10)
space group	$P2_1/c$	2θ scan range, deg	1–50
a, Å	16.540 (8)	scan technique	θ–2θ
b, Å	16.690 (8)	data collected	5405
c, Å	13.910 (9)	scan width, deg	2
β, deg	110.64 (4)	unique data with $I > 2\sigma(I)$	3374
V, $Å^3$	3593	std rflctns	3
Z	8	LS parameters	552
d(calcd), $g \cdot cm^{-3}$	1.60	data/parameters	552/3370
d(obsd), $g \cdot cm^{-3}$	1.57	R, % (F_o)	5.7
cryst color	orange	R_w, % (F_o)	6.7

techniques and refined by full-matrix least-squares methods. Disorder was encountered for the BF_4^- groups, as usual, and unusually large thermal ellipsoins for F atoms were observed. In the final refinement anisotropic thermal parameters were used for non-hydrogen atoms. The final difference Fourier map was essentially featureless with no peaks greater than 0.3 e $Å^{-3}$. All computations were performed on a PDP 11/34 computer with the aid of the Structure Determination Crystallographic Program Library obtained with the purchase of the X-ray equipment.

Reaction of 6 with CO To Give 7. A 10-mL round-bottomed flask equipped with a stirring bar was flame-dried under a flow of nitrogen. After being cooled to room temperature, the flask was charged with diphos complex **6** (500 mg, 0.625 mmol) and 5 mL of CH_2Cl_2. The flask was purged with CO and then placed under 1 atm of CO by means of a balloon filled with CO and stirred at room temperature for 3 h. During this time the solution turned from deep amber to bright yellow. The solution was evaporated to dryness at room temperature on a rotary evaporator to give a yellow solid. Recrystallization from CH_2Cl_2/Et_2O afforded 476 mg (92%) of **7** as a yellow, crystalline methylene chloride solvate: mp 149–151 °C; IR (CH_2Cl_2, cm^{-1}) 260, 1711, 1666; 270-MHz ^1H NMR ($CDCl_3$) δ 7.93–7.04 (m, 24 H), 5.31 (s, 2 H), 3.48–2.84 (m,4 H), 1.57 (s, 3 H). Anal. Calcd for $CoC_{39}H_{33}O_3P_2Cl_2NBF_4$: C, 54.97, H, 4.01; N, 1.69. Found: C, 55.07; H, 4.12; N, 1.73.

Synthesis of Dimethylglyoxime–PPh_3 Complex 8. Phthaloylcobalt complex **1** (2.0 g, 2.7 mmol), dimethylglyoxime (340 mg, 2.9 mmol), and 26 mL of reagent grade acetonitrile were refluxed with stirring under a nitrogen atmosphere until all of the starting material had solubilized. The solution was cooled and the CH_3CN removed on a rotary evaporator to leave a solid residue that was triturated with Et_2O to afford 1.6 g (100%) of complex **8** as a greenish gold solid: mp 203–204 °C (CH_3CN/Et_2O); IR (CH_2Cl_2, cm^{-1}) 1635, 1604, 1572, 1488; 270-MHz ^1H NMR ($CDCl_3$) δ 13.59 (s, 2 H), 7.57–7.49 (m, 2 H), 7.36–7.24 (m, 5 H), 7.24–7.10 (m, 12 H), 2.01 (s, 6 H). Anal. Calcd for $CoC_{30}H_{27}ClN_2O_4P$: C, 59.56; H, 4.50; N, 4.63. Found: C, 59.55; H, 4.63; N, 4.74.

Synthesis of Dimethylglyoxime–Pyridine Complex 9. Phthaloylcobalt complex **1** (10.0 g, 0.013 mmol) was slurried in 65 mL of distilled pyridine under nitrogen at room temperature for 2 h to produce a very insoluble bright orange solid. Addition of 250 mL of Et_2O completed the precipitation of the solid, and it was collected by suction filtration using an Et_2O wash to afford 4.55g of an orange powder; IR (KBr) 1640 cm^{-1}. The orange solid (734 mg, 1.91 mmol), dimethylglyoxime (221 mg, 2.00 mmol), and 19 mL of CH_3CN were refluxed with stirring under a nitrogen atmoshere until all of the starting materials were solubilized. The solvent was removed on a rotary evaporator, and the solid residue was triturated with Et_2O to afford complex **9** (765 mg, 95%) as a yellow-brown solid: mp 187–188 °C (CH_3CN/Et_2O); IR (CH_2Cl_2, cm^{-1}) 1605, 1570, 1475; 270-MHz ^1H NMR ($CDCl_3$) δ 13.76 (s, 2 H), 8.30 (dd, J = 6 Hz, J = 1.4 Hz, 2 H), 7.91 (dd, J = 5.5 Hz, J = 3.3 Hz, 2 H), 7.49 (overlapping tt, J = 8 Hz, J = 1.4 Hz, 1 H), 7.45 (overlapping dd, J = 5.5 Hz, J = 3.3 Hz, 2 H), 7.03 (dd, J = 8 Hz, J = 6 Hz, 2 H), 2.32 (s, 6 H). Anal. Calcd for $C_{17}H_{17}CoN_3ClO_4$: C, 48.41; H, 4.06; N, 9.97. Found: C, 48.31; H, 4.21; N, 10.05.

Collection of the X-ray Diffraction Data and Solution of the Crystal Structure of (Phthaloyl)Co(dimethylglyoxime)(pyridine)Cl (9). Single crystals of **9** were grown by dissolving a sample in a minimum amount of hot CH_3CN and allowing Et_2O to slowly diffuse into the solution. The experimental data for the X-ray diffraction study are given in Table VI. No absorption correction was necessary (μ = 11.3 cm^{-1}). The structure was solved by Patterson and successive Fourier techniques and refined by full-matrix least-squares methods. In the final refinement anisotropic thermal parameters were used for non-hydrogen atoms. Methyl hydrogens were located from a difference Fourier map; the remaining hydrogen atom parameters were calculated by assuming idealized geometry. Hydrogen atom contributions were included in the structure factor calculations, but their parameters were not refined. The final difference Fourier map was essentially featureless with no peaks greater than 0.3 e $Å^{-3}$. All computations were performed on a PDP 11/34 computer with the aid of the Structure Determination Crystallographic Program Library obtained with the purchase of the X-ray equipment.

Reaction of Dimethylglyoxime Complex 9 with 3-Hexyne at 80 °C (Table I). All reactions were conducted under nitrogen in sealed tubes containing a small magnetic stirring bar and charged with 0.1 mmol of the dimethylglyoxime complex **9**, 0.15 mmol of 3-hexyne, 1.0 equiv of the additives shown in Table I, 0.1 mmol of biphenyl as an internal standard, and 1 mL of CH_2Cl_2. After sealing, the reaction tubes were placed in an oil bath maintained at 80 °C and vigorously stirred. At the indicated times, the tubes were removed from the oil bath and cooled to 0 °C, and a GC aliquot was removed and analyzed. Yields were calculated from gas chromatography peak areas by using internal standard techniques.

Reaction of Dimethylglyoxime Complex 9 with 1-Hexyne at 25 °C (Table II). All reactions were conducted under nitrogen in a flame-dried round-bottomed flask equipped with a small magnetic stirring bar. Dimethylglyoxime complex **9** (42 mg, 0.10 mmol), 1-hexyne (17 μL, 0.15 mmol), the Lewis acid (0.10 mmol), and 1 mL of dichloroethane were stirred at room temperature for 5 h. The reaction mixture was quenched with dilute HCl, vigorously stirred for 1 h, and then extracted into Et_2O. The ether layer was washed with saturated $NaHCO_3$, dried (Na_2SO_4), filtered, and condensed on a rotary evaporator, and the resulting crude product was chromatographed on a short SiO_2 column with 3:2 hexane–Et_2O to give the pure quinone in the yields indicated in Table II. The product was identical with material rigorously characterized in a previous publication.[6]

Preparation of Quinones from Dimethylglyoxime Complex 9 in the Presence of $CoCl_2 \cdot 6H_2O$ and $SnCl_4$. A. $CoCl_2 \cdot 6H_2O$ System. Alkyne (1.5 equiv), complex **9** (1.0 equiv), $CoCl_2 \cdot 6H_2O$(1.0 equiv), and dichloroethane (to make solution 0.1 M in **9**) were refluxed in a round-bottomed flask under nitrogen for 8 h. Workup was the same as that described in the previous section. The naphthoquinones from 1-hexyne, 3-hexyne, ethyl tetrolate, ethyl 1-propynyl ether, and 2,2-dimethyl-3-pentyne were identical with those previously described in ref 6. The menaquinones MK-1 and MK-2 (last two entries in the table) were prepared from the appropriate alkynes and showed IR and ^1H NMR consistent with the literature data.[15] The required alkynes were synthesized as follows. **2-Methyl-2-hept-5-yne.**[16] According

(15) Syper, L.; Kloc, K.; Mlochowski, J. *Tetrahedron* **1980**, *36*, 123.
(16) Koster, R.; Bussman, A.; Schroth, G. *Liebigs Ann. Chem.* **1975**, 2130.

Table VII. Bond Lengths and Angles of 9

molecule 1		molecule 2	
	Distances (Å)		
Co1–Cl1	2.251 (2)	Co2–Cl2	2.253 (2)
Co1–N1	2.015 (6)	Co2–N4	2.024 (6)
Co1–N2	2.026 (6)	Co2–N5	1.998 (7)
Co1–N3	1.960 (6)	Co2–N6	1.969 (6)
Co1–C18	1.871 (8)	Co2–C1	1.863 (8)
Co1–C25	1.860 (8)	Co2C8	1.874 (8)
N1–O1	1.393 (6)	N4–O5	1.380 (7)
N1–C26	1.273 (8)	N4–C29	1.279 (7)
N2–O2	1.376 (6)	N5–O6	1.388 (7)
N2–C27	1.285 (9)	N5–C10	1.287 (8)
N3–C30	1.355 (8)	N6–C13	1.343 (9)
C30–C31	1.347 (9)	C13–C14	1.388 (10)
C31–C32	1.386 (10)	C14–C15	1.350 (10)
C32–C33	1.342 (8)	C15–C16	1.340 (9)
C33–C34	1.369 (8)	C16–C17	1.373 (9)
C34–N3	1.343 (8)	C17–N6	1.324 (8)
C18–O3	1.222 (8)	C1–O7	1.222 (8)
C18–C19	1.499 (8)	C1–C2	1.494 (9)
C19–C20	1.371 (9)	C2–C3	1.384 (10)
C20–C21	1.363 (10)	C3–C4	1.398 (11)
C21–C22	1.382 (11)	C4–C5	1.363 (11)
C23–C24	1.398 (8)	C5–C6	1.353 (11)
C24–C25	1.480 (8)	C6–C7	1.374 (9)
C25–O4	1.239 (8)	C8–O8	1.221 (8)
C26–C27	1.485 (9)	C9–C10	1.479 (8)
C26–C28	1.482 (9)	C9–C11	1.492 (10)
C27–C29	1.473 (9)	C10–C12	1.489 (10)
	Angles (deg)		
	Around Cobalt		
Cl1–Co1–N1	90.5 (6)	Cl2–Co2–N4	92.1 (6)
Cl1–Co1–N2	90.5 (6)	Cl2–Co2–N5	90.3 (7)
Cl1–Co1–N3	176.9 (6)	Cl2–Co2–N6	176.3 (6)
Cl1–Cl1–C18	86.5 (7)	C12–Co2–C1	87.6 (7)
N1–Co1–N2	75.9 (8)	N4–Co2–N5	76.5 (8)
N1–Co1–N3	91.1 (7)	N4–Co2–N6	91.6 (7)
N1–Co1–C18	98.7 (8)	N6–Co2–C1	97.2 (8)
N2–Co1–N3	92.4 (7)	N4–Co2–N6	91.2 (8)
N2–Co1–C18	173.9 (8)	N5–Co2–C1	173.3 (7)
N3–Co1–C18	90.6 (8)	N6–Co2–C1	91.3 (8)
	Within Ligands		
O1–N1–C26	116.0 (8)	O5–N4–C9	116.3 (8)
O2–N2–C27	116.7 (7)	O6–N5–C10	115.9 (8)
C30–N3–C34	116.0 (8)	C13–N6–C17	116.7 (9)
O3–C18–C19	121.6 (8)	N5–O6–C10	122.0 (8)
C18–C19–C20	126.4 (9)	O7–C1–C2	121.6 (8)
C18–C19–C24	112.4 (8)	C1–C2–C3	125.3 (9)
C20–C19C24	121.3 (7)	C1–C2–C7	114.0 (9)
C19–C20–C21	119.5 (10)	C3–C2–C7	120.6 (9)
C20–C21–C22	120.0 (10)	C3–C3–C4	117.6 (9)
C21–C22–C23	121.6 (8)	C3–C4–C5	120.8 (10)
C22–C23–C24	118.3 (8)	C4–C5–C6	121.4 (9)
C19–C24–C23	119.3 (7)	C5–C6–C7	119.6 (10)
C19–C24–C25	113.9 (7)	C2–C7–C6	119.8 (10)
C23–C24–C25	126.8 (7)	C2–C7–C8	112.5 (8)
C24–C25–O4	120.3 (7)	C6–C7–C8	127.6 (8)
N1–C26–C27	112.8 (8)	N4–C9–C10	113.3 (7)
N1–C26–C28	124.5 (8)	N4–C9–C11	125.4 (9)
C27–C26–C28	122.6 (9)	C10–C9–C11	121.2 (9)
N2–C27–C26	113.3 (8)	N5–C10–C9	113.1 (8)
N2–C27–C29	124.5 (9)	N5–C10–C12	125.2 (9)
C26–C27–C29	122.1 (9)	C9–C10–C12	121.7 (9)
N3–C30–C31	123.8 (7)	N6–C13–C14	121.9 (9)
C30–C31–C32	118.0 (9)	C13–C14–C15	120.1 (9)
C31–C32–C33	120.0 (8)	C14–C15–C16	117.9 (9)
C32–C33–C34	118.9 (8)	C15–C16–C17	120.4 (8)
N3–C34–C33	123.2 (7)	N6–C17–C16	120.0 (8)

to the procedure of Yamamoto for coupling of acetylides with allylic halide,[17] LiI was prepared by gradual addition of MeI (6.85 mL, 110 mmol) to *n*-BuLi in hexanes (56.25 mL of 1.6 M, 90 mmol) contained in a flame-dried 250-mL round-bottomed flask under a nitrogen atmosphere at 0 °C. A white precipitate of LiI formed. The hexanes were removed under vacuum and dissolved in 90 mL of THF. In a separate flame-dried, three-neck, 250-mL round-bottomed flask equipped with a magnetic stir bar and maintained under N_2 was added 60 mL of THF and 2 mg of triphenylmethane. The flask was cooled to −78 °C in a dry ice–acetone bath, *n*-BuLi in hexanes (37.50 mL of 1.6 M, 60 mmol) was added dropwise via an addition funnel, and propyne was then bubbled through the solution until the red color of the indicator disappeared. At this time the THF solution of LiI was added to the propynyllithium maintained at −78 °C. Prenyl chloride (available from Alfa) (9.40 g, 90 mmol) was added, and the mixture was allowed to warm to room temperature and then was refluxed for 1 h. After being cooled to room temperature, the reaction was diluted with 750 mL of H_2O and extracted with Et_2O. The ether layer was washed repeatedly with H_2O to remove THF and then washed with saturated NH_4Cl and dried (Na_2SO_4). Filtration followed by careful removal of ether on a rotary evaporator and distillation gave 2-methyl-2-heptene-5-yne[17] in 84% yield. **Methylgeranylacetylene** was prepared by an identical procedure from geranyl chloride[18] in 90% yield and showed the following ^1H NMR data at 200 MHz in $CDCl_3$: δ 5.18 (br t, 1 H), 5.10 (m, 1 H), 2.84 (br d, 2 H), 2.02 (m, 4 H), 1.78 (t, J = 2 Hz, 3 H), 1.68 (br s, 3 H), 1.66 (2 overlapping br s, 6 H).

B. $SnCl_4$ System. Alkyne (1.5 equiv) and **9** (1.0 equiv) were added to a flame-dried, round-bottomed flask containing enough dichloroethane to make the reaction 0.1 M in **9**. Then 1 equiv of $SnCl_4$ was added, and the reaction mixture was allowed to stir at room temperature for 7 h. After addition of dilute HCl and stirring for 1 h, the reaction was subjected to the same workup as described above for the results in Table II.

Reaction of 9 with PPh_3 To Give 8. Dimethylglyoxime complex **9** (105 mg, 0.25 mmol), PPh_3 (197 mg, 0.75 mmol), and 2 mL of CH_3CN were heated at reflux with stirring for 15 min. After the solution was cooled to room temperature slow, dropwise addition of Et_2O resulted in precipitation of **8** as a gold solid (130 mg, 86%) which was identical with a previously prepared sample.

Reaction of 9 with $Et_4N^+Cl^-$ To Give 10. $Et_4N^+Cl^-$ (173 mg, 1.0 mmol) and **9** (420 mg, 1.0 mmol) were stirred in 5 mL of acetone at room temperature under nitrogen for 72 h. The deep red precipitate that formed was filtered, washed with Et_2O, and dried: IR (KBr, cm^{-1}) 1600, 1575; 270-MHz ^1H NMR (CD_2Cl_2) δ 14.23 (s, 2 H), 7.93 (m, 2 H), 7.52 (m, 2 H), 2.72 (q, J = 7.5 Hz, 8 H), 2.44 (s, 6 H), 1.07 (tt, J = 7.2 Hz, J = 1.6 Hz, 12 H). This coupling pattern for the tetraethylammonium ion is precedented.[19] Anal. Calcd for $C_{20}H_{32}CoN_3Cl_2O_4$: C, 47.25; H, 6.35. Found: C, 47.29; H, 6.11.

Acknowledgment. This investigation was supported by PHS Grants CA 26374 and CA 40157 awarded by the National Cancer Institute, DHHS.

Registry No. **1**, 75895-97-5; **6**, 101565-38-2; **6** · CH_3CN, 101565-39-3; **7**, 101565-41-7; **8**, 101565-42-8; **9**, 101565-43-9; **10**, 101565-45-1; EtC≡CEt, 928-49-4; *n*-BuC≡CH, 693-02-7; MeC≡CCO_2Et, 4341-76-8; EtC≡COEt, 14272-91-4; MeC≡CBu-*t*, 999-78-0; MeC≡CCH_2CHCMe_2, 58275-81-3; (*E*,*E*)-MeC≡C-$[CH_2CHCMeCH_2]_2$H, 76672-76-9; 2,3-diethyl-1,4-naphthoquinone, 2397-59-3; 2-butyl-1,4-naphthoquinone, 34491-88-8; 2-(ethoxycarbonyl)-3-methyl-1,4-naphthoquinone, 68749-79-1; 2-ethoxyl-3-ethyl-1,4-naphthoquinone, 55025-03-1; 2-*tert*-butyl-3-methyl-1,4-naphthoquinone, 75909-62-5; 6-methyl-hept-2-yne, 957-78-8; 2-methyl-3-[(*E*,*E*)-3,6-dimethylhepta-2,5-diene-1-yl)-1,4-naphthoquinone, 1163-13-9.

Supplementary Material Available: Tables of structure factors and positional and thermal parameters for **6** and **9** (41 pages). Ordering information is given on any current masthead page.

(17) Yatagi, H.; Yamamoto, Y.; Maruyama, K. *Chem. Lett.* **1980**, 669.

(18) Snyder, E. I. *J. Org. Chem.* **1972**, *37*, 1466.

(19) Jackman, L. M.; Sternhell, S. *Nuclear Magnetic Resonance Spectroscopy in Organic Chemistry*, 2nd ed.; Pergamon: London, 1969; pp 354–355.